JOURNAL OF CATALYSIS **167,** 464–469 (1997)
ARTICLE NO. CA971602

High-Pressure Temperature-Programmed Reduction of Sulfided Catalysts

Franck Labruyère,* Michel Lacroix,* Daniel Schweich,† and Michèle Breysse*

*Institut de Recherches sur la Catalyse, 2 Avenue Albert Einstein, 69626 Villeurbanne Cedex, France; and †Laboratoire de Génie des Procédés Catalytiques, CPE–Lyon, BP 2077, 43 Boulevard du 11 Novembre, 69616 Villeurbanne Cedex, France

Received June 7, 1996; revised January 6, 1997; accepted January 6, 1997

Temperature-programmed reduction (TPR) of solids materials is a widely used technique of characterization in heterogeneous catalysis. So far all studies dealing with this technique have been carried out at ambient or subambient pressure. Because most catalytic processes are performed at higher hydrogen pressures, the impact of this technique could be enhanced by the development of a new generation of equipment working under conditions approaching those used in reality. This work describes a new experimental temperature-programmed reduction set-up working at hydrogen pressures above 1 atm. Basic hydrodynamic considerations have been employed for correcting the signal from the variations of the residence time distribution of the molecules in the reactor. Model and industrial sulfide catalysts were studied at various pressures. When the raw signals are suitably corrected, it appears that the hydrogen pressure does not influence the TPR patterns. © 1997 Academic Press

INTRODUCTION

It is well established that transition metal sulfides (TMS) are efficient catalysts for performing several reactions such as hydrodesulfurization, hydrodenitrogenation, and hydrogenation involved in the hydrotreating processes. Extensive works devoted to the understanding of these materials have shown evidence that their catalytic properties are closely related to the presence of coordinatively unsaturated sites (CUS) formed upon partial reduction of the catalyst surface under the experimental conditions utilized for the measurement of their catalytic properties (1–6). The activity and the adsorbing properties of such solids were found to be drastically dependent on the sulfur-to-metal ratio (3, 6). Although the latter research has improved the knowledge about TMS properties, they were performed at atmospheric pressure, whereas hydrotreating processes require hydrogen pressures about 10–60 bar at least. Knowing that the reduction of a solid catalyst can be pressure dependent, this could limit the impact and the pertinence of the results cited above.

The temperature-programmed reduction (TPR) technique has been widely used to study the stability of solids and the decomposition of catalyst precursors in the presence of hydrogen (7, 8). In a typical TPR run hydrogen is fed to a fixed amount of solid at a temperature low enough to prevent reaction. The temperature of the solid is then linearly increased and depending on the nature of the solid under study the rate of the reaction is recorded by measuring the changes in reactant or product concentrations in the exhaust gas. For sulfide catalysts, the H_2S formation or the hydrogen consumption can be detected using appropriate detectors (6, 9). However, when hydrogen is analyzed, only low partial pressures should be employed in order to precisely determine variations in concentration at the reactor outlet excluding high pressure studies. By contrast, measuring the H_2S concentrations at the inlet and the outlet of the reactor gives accurate production rates related to the catalyst reduction process only.

The aim of this work was to develop a TPR reactor working at pressures as high as those currently used for hydrotreating processes, to establish a method for correcting the raw TPR signal from hydrodynamic phenomena, and to test the method with model and industrial catalysts.

EXPERIMENTAL

Catalysts and Materials

Alumina-supported Ru, Mo, and CoMo sulfides were used as model compounds. The Ru-based solid was used because it can be completely reduced at moderate temperature (10). It was prepared by impregnation of a γ-alumina support (BET area 236 m^2/g, pore volume 0.6 cm^3/g) by an aqueous solution of $RuCl_3$. The amount of Ru deposited on the support was 7 wt%. The Mo-based solids were the EUROCAT samples designed for standard testing procedures (11–14). Prior to the sulfidation process, the catalysts were crushed and sieved to an average particle size of 100 μm (80–120 μm). The Mo (9% of Mo) and CoMo (9% of Mo and 2.4% of Co) catalysts were sulfided in a flow microreactor at 673 K for 4 h in a 15% H_2S–85% H_2 mixture at atmospheric pressure. The Ru catalyst was sulfided at 673 K

0021-9517/97 $25.00

in an 15% H_2S–85% N_2 atmosphere ($P = 1$ bar) in order to avoid the intermediate formation of a metallic phase which is difficult to sulfide (15). After sulfidation the solids were cooled to room temperature in the presence of the sulfur-containing atmosphere, flushed with an oxygen-free nitrogen flow, and stored in sealed bottles. High-purity hydrogen (99.995%) from Air Liquide was used without any further purification.

TPR Unit

The simplified scheme of the TPR unit is shown in Figs. 1 and 2. It consists of a homemade tubular upflow fixed-bed reactor. Tubing located below the catalytic bed was built with conventional 316 stainless steel, while the top part of the set-up was constructed with Teflon-coated 316 stainless steel hose connectors in order to avoid any consumption of H_2S by the system. The reactor was designed using a high-temperature sulfur-resistant material (AISI 310 stainless steel; internal diameter 8.9 mm, external diameter 13.5 mm). Nevertheless, corrosion still causes severe problems of stability of the material toward H_2S even at temperatures as low as 473 K whatever the H_2S concentration flowing in it. In order to avoid any H_2S consumption due to the reactivity of this compound with the walls of the reactor, the heated part of the set-up was protected by adding an inner quartz tube which diameter (external diameter 8 mm) has been adjusted in order to minimize the resulting dead volume between both tubings. A sulfur-resistant O-ring allows this inner tube to be hung inside the stainless-steel reactor. By screwing the swagelok-type nut tight this crushable O-ring ensures a pressure drop large enough to force hydrogen to flow in the internal tube only. The catalyst bed (about 15 mm high) is located between two quartz wool plugs. Total pressure was accurately controlled with an electronic WEST 3810 controller which permits a hydrogen pressure ranging from 10 to 70 bar. A set of three ports valves allows this pressure controller to be bypassed, allowing TPR experiments to be run at atmospheric pressure.

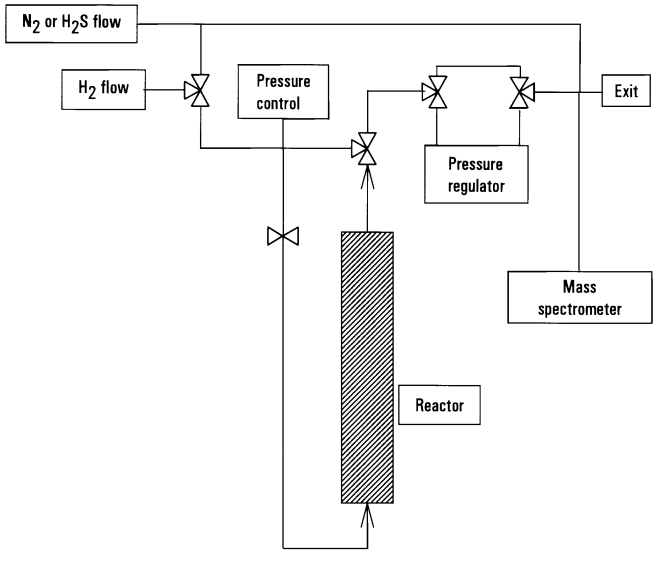

FIG. 1. TPR unit. The arrows indicate the gas flow direction.

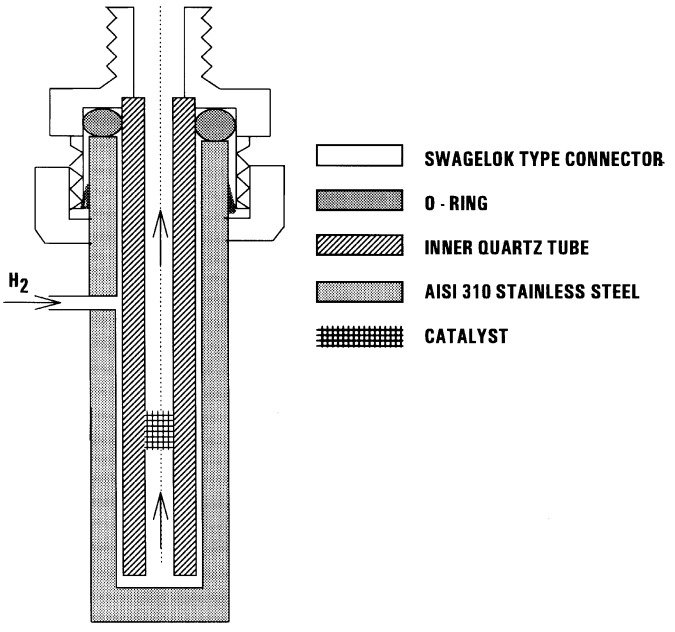

FIG. 2. Expanded view of the swagelok type mounting system. Arrows point in flow direction.

Analytical System

The H_2S released during a run was analyzed by a mass spectrometer (FISONS Instruments) equipped with a quadrupole analyzer (VG analyzer) working in Faraday mode. The gas was continuously sampled using a silica capillary tube heated at 353 K. To avoid a too large increase of the partial pressure into the ionization chamber, the hydrogen flow (slow to be pumped off) was diluted with nitrogen ($N_2 : H_2 = 10 : 1$) at the exit of the pressure controller. The Faraday detector was calibrated with diluted H_2S at a composition close to that observed during a TPR experiment.

Typical Experimental Procedure

In a typical TPR run, 0.2 g of sulfided catalyst was loaded into the inner quartz tube. The reactor was then purged with a nitrogen flow (30 $cm^3\ min^{-1}$) at room temperature until the *m/z* signal relative to oxygen became negligible. Nitrogen was then replaced by hydrogen and the hydrogen pressure was left to reach the desired value. The temperature of the reactor was increased progressively from room temperature to 1073 K using a heating rate of 2 $K\ min^{-1}$. The temperature was measured using a K-type thermocouple. To avoid corrosion, the thermocouple was placed in a

well inserted close to the catalytic bed. Using a heating rate of 2 K min^{-1}, the temperature difference between the catalyst and the well was estimated to be less than 2 K either under a hydrogen pressure of 1 or 31 bar. The temperature and the H_2S signal ($m/z = 34$) were recorded every 60 s.

RESULTS AND DISCUSSIONS

Figure 3 shows a typical TPR profile of an alumina-supported ruthenium sulfide reduced at atmospheric pressure and at 31 bar. Every peak represents a distinct reduction process involving a particular chemical component of the solid. For a given catalyst, the position of the different peaks may change depending on the operating variables, i.e., heating rate, concentration, and flow rate of the reducing gas, amount of reducible species, mass of solid (16). For instance, an increase of heating rates and of catalyst weight loading usually shift peak positions toward higher temperatures, while the concentration of the reducing gas has an opposite effect. The influence of these experimental parameters on peak positions may be important since variations of about 40 K were observed by these authors for the reduction of nickel oxide particles. Therefore, all these running parameters were kept constant and only the pressure was changed in order to examine properly the effect of hydrogen pressure on the reducibility of the solid. However, as shows in Fig. 3 when increasing pressures are applied, peak positions are shifted toward longer times since the residence time distribution (RTD) of a flow reactor is pressure dependent. At a given mass flow rate of the gas, the higher the pressure is, the larger the mean residence time is.

Measurement of the residence time distribution (see below) yields the mean residence time $\tau(P)$ of the gas according to the pressure P. The top curve of Fig. 3 is obtained by translating the middle curve by the difference $\tau(31)-\tau(1)$.

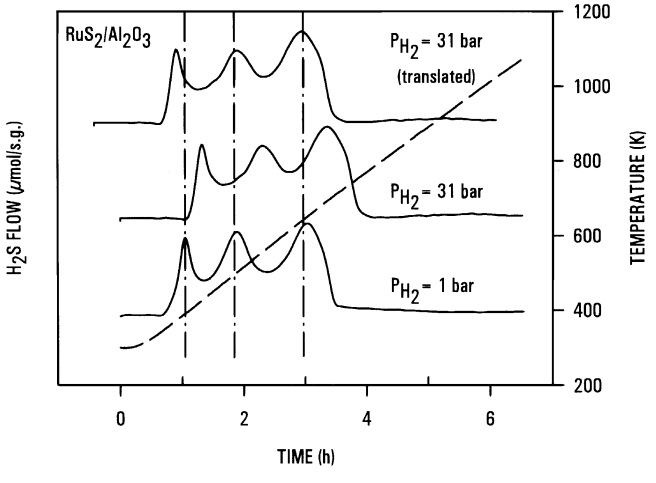

FIG. 3. TPR profile of an alumina-supported ruthenium sulfide for 1 and 31 bar hydrogen pressures.

It is seen that this simple correction does not superimpose the profiles at the two pressures. Consequently, one may wonder whether this shift is due to the sensitivity of the chemical process to pressure or to residual hydrodynamic effect.

The Correction Procedure

The RTD was obtained by the pulse method according to the procedure proposed by Levenspiel (17). A pulse of the inner tracer (0.5 cm^3 of Ar) was quickly injected into the reactor close to the catalytic bed inlet, and the response $C(t)$ was recorded by the mass spectrometer. Figure 4 illustrates the results obtained for various hydrogen pressures. At atmospheric pressure ($P = 1$), the RTD is close to the inlet pulse. This indicates that the flow pattern in the catalyst bed and downstream does not affect the TPR profile. Conversely, at higher pressures ($P = 11$, 21, or 31 bar), the RTD shifts toward larger time and broadens. These curves are typical of a dispersed plug flow which is characterized by the mean residence time τ and a Péclet number Pe at the corresponding pressure. These two parameters are obtained from Eqs. [1], [2], and [3]:

$$\tau = \frac{\int_0^\infty t \times E(t)dt}{\int_0^\infty E(t)dt}, \quad E(t) = \frac{C(t)}{\int_0^\infty C(t)dt} \qquad [1]$$

$$\sigma^2 = \frac{1}{\tau^2}\int_0^\infty (t-\tau)^2 E(t)dt, \qquad [2]$$

where $E(t)$ is the RTD and σ^2 is the reduced variance of the distribution which is related to the Péclet number by

$$\sigma^2 = \frac{2}{\mathrm{Pe}} + \frac{n}{\mathrm{Pe}^2}. \qquad [3]$$

In Eq. [3], n depends on the nature of the boundary conditions used when modeling the dispersed plug flow (17–19). In most situations, Pe is greater than 20 and the second term of [3] can be neglected. Equations [1] and [2] are used to calculate τ and the reduced variance from the experimental RTD, while [3] gives Pe which ranges from 50 at $P = 1$ bar down to 37 at 31 bar. These values suggest that the reactor deviates significantly from the ideal plug flow behavior.

Assuming an open–closed dispersed plug flow reactor, the Fourier transform $\overline{E}(\nu)$ of the RTD curves can be calculated according to Eq. [4] proposed by Villermaux (19):

$$\overline{E}(\nu) = \frac{2\exp(\mathrm{Pe}(1-q)/2)}{1+q}, \quad q = \sqrt{1+\frac{8i\pi\nu\tau}{\mathrm{Pe}}}. \qquad [4]$$

Using a standard fast Fourier transform algorithm the RTD in the time domain $E(t)$ can be calculated taking into account the experimental values of τ and Pe. The computed RTDs are represented in Fig. 4A (dotted lines). The results

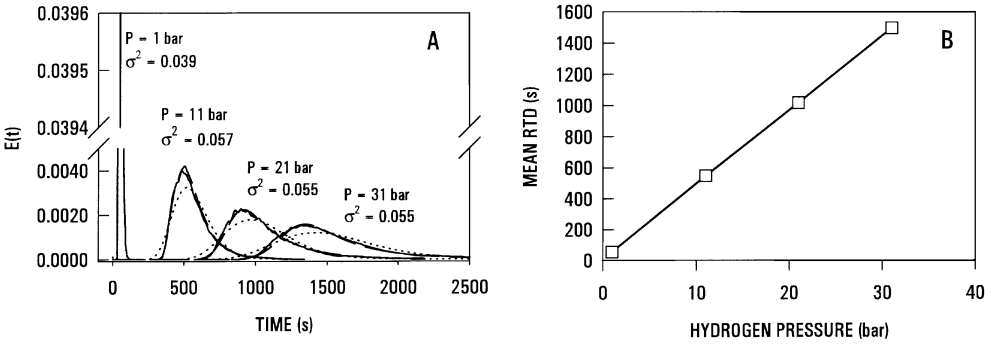

FIG. 4. (A) Stimulus response of the reactor for various hydrogen pressures. Solid lines, experimental data; dotted lines, computed data using Eqs. [4] and [7]; dashed lines, computed data using Eqs. [5] and [7]. (B) Variation of the mean residence time τ with hydrogen pressure.

indicate that the computed curves reproduce the mean location of the experimental $E(t)$ curves reasonably well. However, this modeling procedure does not precisely account for the experimental tailing. According to Levenspiel (17), tailing may arise from the presence of a relatively stagnant phase inside the unit. In these deadwater regions the tracer enters and leaves with a low transfer kinetic. To improve the fitting of the RTD curves, Eq. [4] has been modified into [5] in order to take into account this slow interchange effect between the mobile and stagnant phase.

$$\overline{E}(\nu) = \frac{2\exp(\mathrm{Pe}(1-q)/2)}{1+q},$$
$$q = \sqrt{1+\frac{8i\pi\nu\tau}{\mathrm{Pe}}\frac{1}{1+K'}\left(1+\frac{K'}{1+t_m(2i\pi\nu)}\right)}, \quad [5]$$

where t_m represents the time constant of the mobile-stagnant phase transfer, and $K'/(1+K')$ is the fraction of stagnant vessel volume.

The use of the parameters $K'=0.1$, $\mathrm{Pe}=80$, and $t_m=80$, 200 and 300 s for $P=11$, 21, and 31 bar, respectively, allows one to properly depict the experimental RTD curves (Fig. 4A). Since the computed curves are now almost superposed to the experimental ones. It should be mentioned that no physical significance are attached to these fitting parameters. They only allow a good modeling of the experimental data.

The TPR profiles are then corrected for the hydrodynamic phenomena using standard results of the system dynamics (20). The observed signal TPR_0 can be considered as the convolution of an ideal and corrected signal, TPR_i with the RTD $E(t)$:

$$\mathrm{TPR}_0(t) = \mathrm{TPR}_i(t) * E(t) = \int_0^t \mathrm{TPR}_u E(t-u)du. \quad [6]$$

In the Fourier domain, Eq. [6] becomes

$$\overline{\mathrm{TPR}_0}(\nu) = \overline{\mathrm{TPR}_i}(\nu)\overline{E}(\nu), \quad [7]$$

where $\overline{E}(\nu)$ is the Fourier transform of the RTD and ν is the frequency.

Knowing Pe and τ from the experimental RTD, Eqs. [4] or [5] and [7] are solved for $\mathrm{TPR}_i(t)$ using a standard fast Fourier transform algorithm. In the next sections the observed $\mathrm{TPR}_0(t)$ and corrected $\mathrm{TPR}_i(t)$ signal are compared and discussed.

Ruthenium Sulfide Supported on Alumina

The TPR pattern reported in Fig. 5 contains three peaks. The total sulfur amount corresponds to a sulfur-to-metal ratio of 2.4–2.5. The area underneath each component allows the determination of the amount of each sulfur species. Previous work has shown that the elimination of the sulfur corresponding to the first peak leads to the stoichiometric RuS_2 phase. By analogy with the data reported by Mangnus *et al.*, this peak could be related to the presence of overstoichiometric S_x retained by the solid surface during the sulfiding procedure (6, 21). The second peak has been

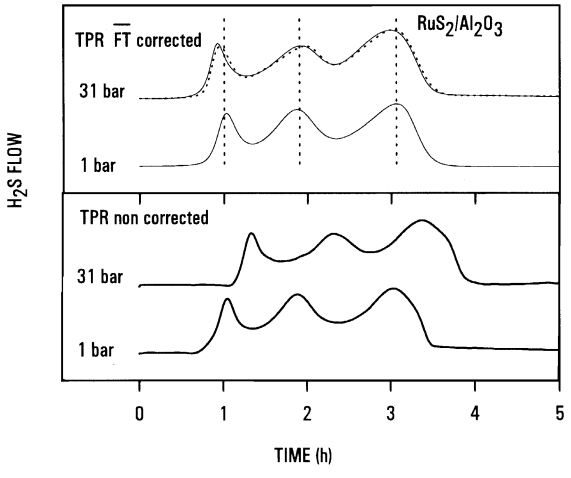

FIG. 5. Corrected and noncorrected TPR profiles of an alumina-supported ruthenium sulfide. Solid lines, corrected profiles using Eqs. [4] and [7]; dotted lines, corrected profiles using Eqs. [5] and [7].

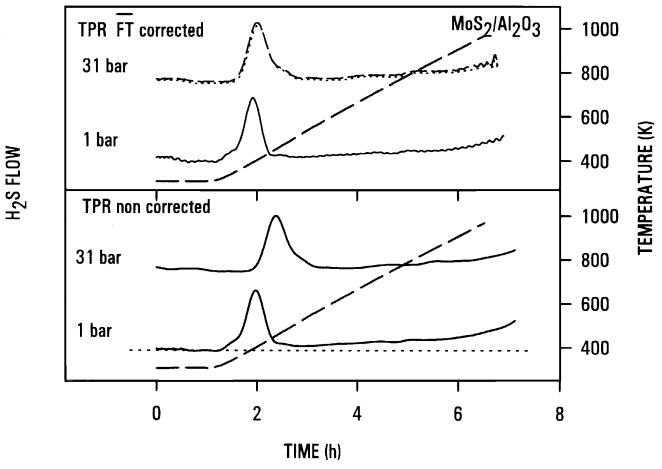

FIG. 6. Corrected and noncorrected TPR profiles of an alumina-supported molybdenum sulfide. Solid lines, corrected profiles using Eqs. [4] and [7]; dotted lines, corrected profiles using Eqs. [5] and [7].

ascribed to the removal of surface sulfur anion while the third peak corresponds to bulk sulfur elimination leading to the metallic ruthenium phase (6, 22). The bottom TPR signals of Fig. 5 are the same as in Fig. 3, while the top profiles concern the corrected TPR signal using Eqs. [4] or [5] and [7]. Both methods lead to similar profiles within experimental errors. This result is not surprising because Eq. [5] differs from [4] only by an additional correcting factor. It is seen that the proposed correction method gives nearly the same curves irrespective of the pressure, indicating that hydrogen pressure does not affect the reduction of the ruthenium-based catalyst. The reduction process involves several steps, i.e., removal of weakly bonded sulfur species and formation of anionic vacancies, adsorption of hydrogen and reaction with surface sulfur anions, hydrogen diffusion into the particle core and desorption of H_2S. According to the observed data the amount of adsorbed hydrogen is already large enough at atmospheric pressure to perform the solid reduction. This behavior suggests that the number of coordinatively unsaturated sites is determined mostly by the temperature and not by the hydrogen pressure.

Molybdenum Sulfide Supported on Alumina

Figure 6 presents the results obtained on the Mo catalysts. Mainly, two domains of H_2S removal are observed. These profiles exhibit a sharp peak below 473 K ($t < 3$ h) followed by a slow reduction process which leads to a continuous H_2S production in a temperature range between 473 and 1000 K. The assignment of the species leaving the catalyst surface is more delicate than for ruthenium sulfide. However, two different models have been proposed to explain the TPR profile of molybdenum containing catalyst. The low-temperature peak could be ascribed either to the presence of overstochiometric S_x species formed by decomposition of H_2S in the micropores during the sulfidation of the solid or to the elimination of weakly bonded SH groups which could be present along the edges of a fully saturated slab of the lamellar structure of MoS_2 (21, 23, 24). Taking into account that the elimination of basal sulfur ions leading to a complete desulfurization of the solid requires temperature as high as 1100–1300 K, the low reduction process is believed to be associated to more strongly bonded S^{2-} ions but still located at the edge structure. Whatever the exact nature of the removable species, mild reduction (for $T < 773$ K) should create only edge vacancies which are recognized to be the active HDS sites. As shown in Fig. 6, an increase of hydrogen pressure does not affect the corrected TPR profile and the amount of sulfur removed under 31 bar is only 8% higher than at atmospheric pressure. Moreover, the observed profiles closely resemble to those already reported in Refs. (21), (23), and (24), recorded at 1 bar and using subatmospheric hydrogen pressures (hydrogen diluted in an inert gas). The reduction mechanism is thus again independent of the hydrogen pressure.

Cobalt Molybdenum Sulfide Supported on Alumina

The TPR patterns reported on Fig. 7 differ significantly from those of MoS_2/Al_2O_3 since two extra peaks are detected in the low-temperature region as well as another one at about 800–900 K. From a structural point of view such a catalyst consists on small MoS_2 slabs in which a fraction of the cobalt ions is linked to their edges by bridging sulfur ions. Besides this mixed "CoMoS" phase, cobalt also exists as small Co_9S_8 particles and the presence of

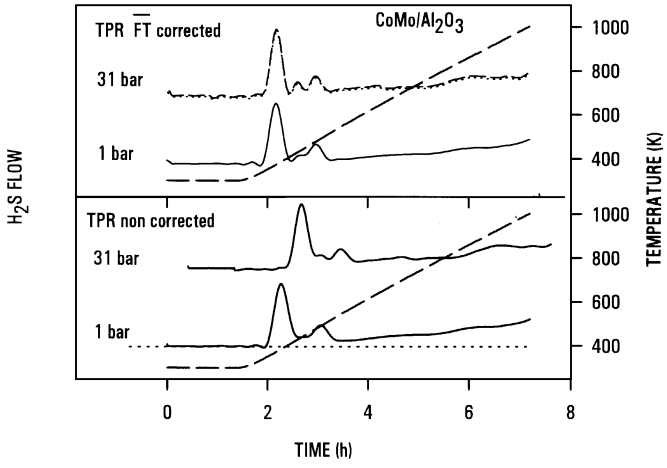

FIG. 7. Corrected and noncorrected TPR profiles of an alumina-supported cobalt–molybdenum sulfide. Solid lines, corrected profiles using Eqs. [4] and [7]; dotted lines, corrected profiles using Eqs. [5] and [7].

some unpromoted MoS_2 crystallites cannot be excluded (25). Accordingly, the presence of various sulfur species having different reactivities are expected. The amount of H_2S removed upon reduction to 31 bar and at the maximum temperature, which can be achieved by the set-up, is only 15% higher than under 1 bar. This difference comes mainly from the higher intensity of the peak observed between 800 and 900 K. However, this species is probably not removed during the catalytic hydrotreating process which takes place at lower temperature. Consequently, the formation of sulfur vacancies is not modified by the hydrogen pressure by industrial operating conditions.

CONCLUSIONS

A set-up allowing high hydrogen pressure reduction of solids has been designed. Examples of TPR patterns obtained have been shown for sulfide catalysts. Nevertheless, the system can be utilized for other kind of catalysts such as oxides and catalysts precursors. A method for correcting the observed TPR profile for the change of the flow pattern with pressure has been proposed. It allows one to ascribe peak shift to real chemical process.

For sulfide catalysts, either ruthenium sulfide- or molybdenum-based catalysts no influence of the hydrogen pressure on the formation of coordinatively unsaturated sites has been observed. This indicates that the amount of hydrogen adsorbed on the surface at atmospheric pressure is large enough to permit the reduction, suggesting that the limiting step is the metal–sulfur bond cleavage.

The validity of the correlation between TPR and catalytic results is then reinforced as well as the site characterizations performed after pretreatment of the solids at low hydrogen partial pressures. Nevertheless, the sites concentration could be related also to the presence of other components such as H_2S in the reactant and product mixtures even with model molecules. The influence of these products is very difficult to address. The present study could be considered as a step forward in the knowledge of sulfide catalysts under more realistic conditions.

This work has shown the potential uses of the TPR technique operating at high hydrogen pressures. The proposed set-up and the methodology employed for correcting the signals from hydrodynamics is not limited to sulfides but can be utilized for other kinds of solid materials.

ACKNOWLEDGMENTS

F.L. is indebted to EURECAT S.A. and the Research Council of the Rhône Alpes district for financial support.

REFERENCES

1. Tanaka, K., *Adv. Catal.* **33**, 99 (1985).
2. Jalowiecki, L., Aboulaz, A., Kasztelan, S., Grimblot, J., and Bonnelle, J. P., *J. Catal.* **120**, 108 (1989).
3. Wambeke, A., Jalowiecki, L., Kasztelan, S., Grimblot, J., and Bonnelle, J. P., *J. Catal.* **109**, 320 (1988).
4. Lacroix, M., Yuan, S., Breysse, M., Dorémieux-Morin, C., and Fraissard, J., *J. Catal.* **138**, 409 (1992).
5. Jobic, H., Clugnet, G., Lacroix, M., Yuan, S., Mirodatos, C., and Breysse, M., *J. Am. Chem. Soc.* **115**, 3654 (1993).
6. Lacroix, M., Mirodatos, C., Breysse, M., Décamp, T., and Yuan, S., *in* "Proceedings, 10th International Congress on Catalysis, Budapest, 1992" (L. Guczi, F. Solymosi, and P. Tétényi, Eds.), pp. 597–609. Akadémiai Kiadó, Budapest, 1993.
7. Bhatia, S., Beltramini, J., and Do, D. D., *Catal. Today* **7**(3), (1990).
8. Jones, A., and McNicol, B. D., *in* "Temperature Programmed Reduction for Solid Materials Characterization," Chemical Industries 24. Decker, New York/Basel, 1986.
9. Scheffer, B., Dekker, N. J. J., Mangnus, P. J., and Moulijn, J. A., *J. Catal.* **121**, 31 (1990).
10. de los Reyes, J. A., Vrinat, M., Geantet, C., and Breysse, M., *Catal. Today* **10**(4), 645 (1991).
11. Medici, L., Zwicky, C., and Prins, R., "Proceedings, Europacat 1," p. 976. Montpellier, France, 1993.
12. Ledoux, M., and Peter, A., "Proceedings, Europacat 1," p. 983. Montpellier, France, 1993.
13. van Gestel, J., Leglise, J., and Duchet, J. C., "Proceedings, Europacat 1," p. 984. Montpellier, France, 1993.
14. Breysse, M., Chadwick, D., Decamp, T., Hellgardt, K., and Oen, A., "Proceedings, Europacat 1," p. 993. Montpellier, France, 1993.
15. Knop, O., *Can J. Chem.* **41**, 1838 (1963).
16. Daniele, A., Monti, A. M., and Baiker, A., *J. Catal.* **83**, 323 (1983).
17. Levenspiel, O., *in* "Chemical Reaction Engineering." Wiley, New York, 1962.
18. Levenspiel, O., and Smith, W. K., *Chem. Eng. Sci.* **6**, 227 (1957).
19. Villermaux, J., *in* "Génie de la réaction chimique." Lavoisier, Paris, 1993.
20. van der Laan, T., *Chem. Eng. Sci.* **7**, 187 (1958).
21. Mangnus, P., Riezebos, A., van Langeveld, A. D., and Moulijn, J. A., *J. Catal.* **151**, 178 (1995).
22. Geantet, C., Calais, C., and Lacroix, M., *C. R. Acad. Sci. Paris*, t.315, Série II, 339 (1992).
23. Kasztelan, S., Toulouat, H., Grimblot, J., and Bonnelle, J. P., *Appl. Catal.* **13**, 127 (1984).
24. McGarvey, G. B., and Kasztelan, S., *J. Catal.* **148**, 149 (1994).
25. Prins, R., de Beer, V. J. H., and Somorjai, G., *Catal. Rev. Sci. Eng.* **31**(1&2), 1 (1989).